

Greenland Monthly Temperature Reconstruction Over The Last 10,000 Years

Saiping Jiang

Beijing Normal University

Aizhong Ye (✉ azye@bnu.edu.cn)

Beijing Normal University <https://orcid.org/0000-0003-0821-783X>

Research Article

Keywords: Greenland, Ice core, Temperature reconstruction, Monthly, Climate change

Posted Date: February 16th, 2022

DOI: <https://doi.org/10.21203/rs.3.rs-1325471/v1>

License:   This work is licensed under a Creative Commons Attribution 4.0 International License.

[Read Full License](#)

1 **Greenland monthly temperature reconstruction over the last 10,000 years**

2 **Saiping Jiang¹, Aizhong Ye^{1*}**

3 ¹ State Key Laboratory of Earth Surface Processes and Resource Ecology, Faculty of
4 Geographical Science, Beijing Normal University, Beijing 100875, China

5

6

7

8

9

Prepared for

10

Climate Dynamics

11

February 2022 (original)

12

13

14

15

16

17

18

19

20

21 **Corresponding Author:**

22 **Aizhong Ye**

23 State Key Laboratory of Earth Surface Processes and Resource Ecology, Faculty of

24 Geographical Science, Beijing Normal University, Beijing 100875, China, Tel/Fax:

25 +86-10-58800207; E-mail: azye@bnu.edu.cn

26

27

28
29
30
31
32
33
34
35
36
37
38
39
40
41
42
43
44
45
46
47
48
49
50
51
52
53
54
55
56

Highlight

1. Monthly temperature data over past 10,000 years was reconstructed in Greenland.
2. The temperature of September to May showed a significant increasing trend at the 0.05 level during period 9700 B. C. E. ~ 2019 C.E., and the increasing rate is 0.0017 ~ 0.0058 °C every two decades. However, the temperature of June to August showed a significant decreasing trend, and the decreasing rate is -0.0035 ~ -0.0040 °C every two decades.
3. This study provides guidelines for the study of climate change and Greenland ice sheet mass balance.

Abstract

Greenland is the biggest island in the world, and the area of snow and ice is the second largest in the world, which is only smaller than Antarctic ice sheet. Studying the temperature change of the island is important for ice sheet melting, especially the summer temperature. In this study, we reconstructed monthly temperature data over past 10,000 years using ice core data, meteorological observation data and European reanalysis data, and linear regression equation– residual correction method was used. And the results are as follows: The temperature of September to May showed a significant increasing trend at the 0.05 level during period 9700 B. C. E. ~ 2019 C.E., and the increasing rate is 0.0017 ~ 0.0058 °C every two decades. However, the temperature of June to August showed a significant decreasing trend, and the decreasing rate is -0.0035 ~ -0.0040 °C every two decades. The climate change can be divided into four increasing periods, namely, period 9700 B. C. E. ~ 9600 B.C.E, period 9400 B. C. E. ~ 7720 B.C.E, period 6240 B. C. E. ~ 6000 B.C.E, and 1800 C.E. ~ 2019 C.E., and three decreasing periods, namely, period 9600 B. C. E. ~ 9400 B.C.E, period 6340 B. C. E. ~ 6240 B.C.E. and 6000 B.C.E. ~ 1800 C.E., and one stable periods, namely, 7720 B.C.E. ~ 6340 B.C.E. And the differences of temperature change rate of different altitudes of the same period and month is not obvious. And the temperature change rate in Winter is larger than that in Summer. The dataset can provide data basis for the study of Greenland ice sheet mass balance.

Key words: Greenland· Ice core· Temperature reconstruction· Monthly· Climate change

1. Introduction

Polar glaciers are extremely sensitive to temperature change, the polar glaciers are retreating

57 in different degrees because of global warming. Some studies have shown that there is a polar
58 amplification phenomenon of temperature change in the Arctic, that is, the temperature change in
59 the Arctic is twice that of the global average temperature (Cohen et al., 2014). This amplification
60 phenomenon aggravates the melting of polar glaciers, and the amount of sea ice around the Arctic
61 is further reduced due to climate warming. Greenland is the largest island in the world, and has the
62 second largest ice sheet in the world only after the Antarctic ice sheet. The study of the change
63 characteristics of the ice sheet mass balance in this area can predict and evaluate its impact on the
64 global sea level, which has certain guiding significance for the political, economic and cultural
65 development of the world's coastal countries. Temperature and precipitation are the most basic and
66 important variables in water balance modeling. Temperature not only affects precipitation patterns,
67 but also plays a decisive role in the onset and cessation of ablation. Therefore, the study of
68 temperature change characteristics in Greenland can provide a basis for understanding climate
69 change and further study of water balance change in this area. Most meteorological observation
70 records can only date back to past 150 years, which limits our understanding of long-term climate
71 change (Kobashi et al., 2010). Ice core data extends the temperature records to the past 10,000 years
72 by temperature proxy data.

73 Scientists collected some ice cores samples in Greenland in the 1990s, and then many scientists
74 reconstructed temperature dataset using these ice cores data. Kobashi et al. (2017) reconstructed
75 Greenland Summit temperatures dataset over past 10,000 years using argon and nitrogen isotopes
76 in GISP2 ice core, and they analyzed temperature change characteristic and driver factor influencing
77 temperature change. The reconstructed temperature dataset can better describe temperature change
78 characteristic, such as 9.2 ka event, 8.2 ka event and Holocene Thermal Maximum and so on. And
79 volcanic eruptions are important driving factor to temperature cooling. Johnsen et al. (2001)
80 reconstructed palaeotemperature record from Greenland six ice-core stations using conversion
81 function method between $\delta^{18}\text{O}$ record and temperature, or modeling inversion of the bore
82 temperature profile. The reconstructed results had similar characteristic using different methods.
83 Steffensen et al. (2008) analyzed the last two abrupt warming events around Younger Dryas cooling
84 event using NGRIP, GISP2, GRIP and DYE-3 ice core $\delta^{18}\text{O}$ record. Buizert et al. (2018)
85 reconstructed seasonally temperature change over past 10,000 years by merging ice-core

86 reconstructions with transient climate-model simulations, and analyzed the spatial distribution
87 characteristic of last deglaciation and Holocene temperature. Orbital forcing was the important
88 influence factor for summer temperature, whereas greenhouse gas and AMOC forcings are
89 important influence factors for winter temperatures. Unlike previous studies, Badgeley et al. (2020)
90 used paleoclimate data assimilation method to reconstruct temporal and spatial temperature of
91 Greenland Ice Sheet over the last 20,000 years.

92 Since most of the ice core data are annually data, the current temperature analysis is also
93 focused on annually data, and most of the research is focused on temperature reconstruction of a
94 single ice core site. However, glacier melting mainly occurs in summer, and most of the other
95 seasons are the accumulation stage of glacier energy. Therefore, it is more important to reconstruct
96 monthly temperature datasets in order to better study the characteristics of glacier mass change and
97 glacier melting change. Therefore, this chapter focuses on the reconstruction of the monthly
98 temperature dataset covering the whole island in the past ten thousand years and analyzes the
99 characteristics of the monthly temperature changes in the past ten thousand years, so as to lay a
100 foundation for the further study of the water balance and climate change in Greenland.

101 The specific structure of this chapter is as follows: 2. Study area and data; 3. Methods; 4.
102 Results and discussion; 5. Conclusions.

103 **2. Study area and data**

104 **2.1 Study area**

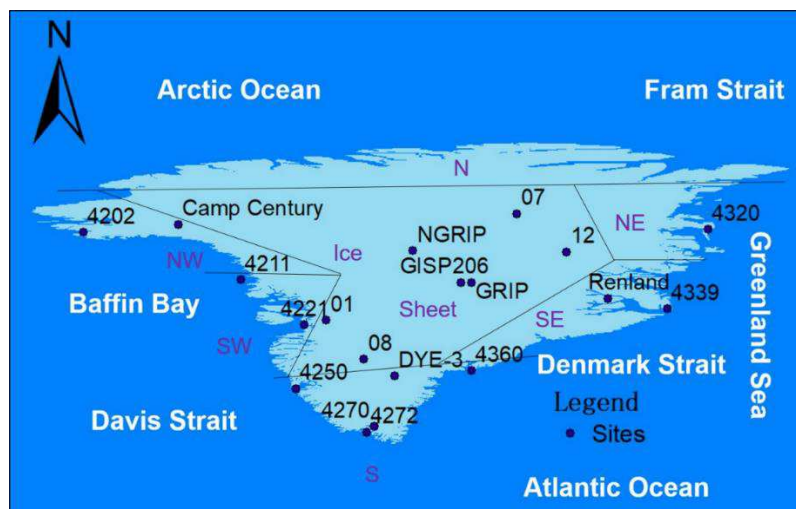
105 Greenland is located at 59°46' N ~ 83°39' N, 11°39' W ~ 73°08' W, and the north-south length
106 and the east-west width of the Island are 2 670 km and 1 050 km, respectively. Greenland is the
107 largest Island in the world, the whole area is 2 166 086 km². 82% of the Island area is covered by ice
108 and snow, and the area of ice and snow is 1.8×10⁶ km², the ice volume is 3.0×10⁶ km³, the max ice
109 thickness is 3 367m. Greenland is surrounded by oceans, and the north, east, west, southeast and
110 southwest part of the Island is surrounded by Arctic Ocean, Greenland Sea, Baffin Bay, North
111 Atlantic Ocean, and Davis Strait, respectively, which is easily affected by sea current. Arctic Ocean
112 and North Atlantic Ocean affect the exchange of cold and warm current of the Island. The capital of
113 Greenland is Nuuk, the total population is 555 877 in 2018. Greenland is Arctic climate, the change
114 of climate is easily affected by ocean-atmosphere General Circulation index, such as Greenland

115 Block Index (GBI), North Atlantic Oscillation (NAO) and so on. The Island can be divided into
116 seven regions. The climate in each region is different. And the temperature in south region is higher
117 than that in north region, the maximum temperature is higher than 10°C in south region, and the
118 minimum temperature may be lower than -40 °C in the north region. And sometimes the temperature
119 in ice sheet is lower than -70 °C in winter. The temperature in the island is easily affected by foehn
120 wind, which can cause drastic changes in temperature.

121 2.2 Meteorological observation data

122 The monthly coastal meteorological observation data in Greenland was downloaded from
123 Danish Meteorological Institute (DMI), and the website is: <https://www.dmi.dk/publikationer/>.
124 There are 9 weather stations used in this study, namely, 4202 Pituffik, 4211 Mitt.Upernavik, 4221
125 Mitt.Ilulissat, 4250 Nuuk, 4270 Mitt.Narsarsuaq, 4272 Qaqortoq, 4320 Danmarkshavn, 4339
126 Ittoqqortoormiit and 4360 Tasiilaq. Because of the bad climate, acquiring the meteorological
127 observation data in Greenland is very difficult, and there were some gaps in this data. To analyze
128 change characteristic of the monthly air temperature, we fill the gaps using Jiang’s Methods (Jiang
129 et al., 2020). And the time span of coastal meteorological data is from 1961 to 2019.

130 The monthly inland meteorological observation data in Greenland was downloaded from this
131 paper “Surface climatology of the Greenland ice sheet: Greenland Climate Network 1995-1999”
132 (Steffen and Box, 2001). And there are five weather stations used in this study, namely, 01 Swiss
133 Camp, 08 DYE-2, 12 NASA-E, 07 TUNU-N and 06 Summit. And the time span of this data is from
134 1995 ~ 2001. Fig. 1 shows the spatial distribution of the coastal and inland weathers stations.



135

136

Fig. 1 Location of weather stations.

137 **2.3 Ice core data**

138 The ice cores data were downloaded from NOAA paleoclimatology data website, and the
139 website is: <https://www.ncdc.noaa.gov/data-access/paleoclimatology-data/datasets>. We used $\delta^{18}\text{O}$
140 to reconstruct temperature change over the past ten thousand years. And there were six ice cores
141 used in this study, namely, Camp century, NGRIP, GRIP, GISP2, Renland and DYE-3. The time
142 resolution of the data is 20 years, and the time span of this data is from 9700 BC to 1960 AD. From
143 Fig. 1, we can see that the distribution of these ice cores is uniform in the whole ice sheet, it means
144 that the data is representative.

145

146 **2.4 European Centre for Medium-Range Weather Forecasts data**

147 We used ERA40 and ERA5 data in this study to extend inland temperature data and acquire
148 temperature spatial distribution information of Greenland, respectively. And the data were
149 downloaded from the following website: [https://apps.ecmwf.int/datasets/data/era40-](https://apps.ecmwf.int/datasets/data/era40-mnth/levtype=sfc/)
150 [mnth/levtype=sfc/](https://apps.ecmwf.int/datasets/data/era40-mnth/levtype=sfc/) and [https://cds.climate.copernicus.eu/cdsapp#!/dataset/reanalysis-era5-land-](https://cds.climate.copernicus.eu/cdsapp#!/dataset/reanalysis-era5-land-monthly-means?tab=overview)
151 [monthly-means?tab=overview](https://cds.climate.copernicus.eu/cdsapp#!/dataset/reanalysis-era5-land-monthly-means?tab=overview), respectively. The time span of ERA40 dataset is from 1958 to 2001,
152 and the data resolution is $0.75^\circ \times 0.75^\circ$, but it was interpolated to $0.125^\circ \times 0.125^\circ$ in this study. The
153 resolution of ERA5 data is $0.1^\circ \times 0.1^\circ$, which spans from 1970 to 2020. Because these datasets cover
154 global area, it's not accurate when used in a specific area. In this study, quantile-Mapping method
155 was used to correct the deviation of temperature data.

156

Table 1 Station information. Lon represents Longitude, Lat represents Latitude, Ele represents Elevation.

Station number	Station name	Lon (°)	Lat (°)	Ele (m)	Time span (Year)	Length(m)	Drilling Time (Year)	Sources
4202	Pituffik	76.53	-68.75	77	1961 ~ 2019	—	—	DMI
4320	Danmarkshavn	76.77	-18.67	11	1961 ~ 2019	—	—	DMI
4211	Mitt.Upernavik	72.78	-56.13	126	1961 ~ 2019	—	—	DMI
4221	Mitt.Ilulissat	69.23	-51.07	29	1861 ~ 2019	—	—	DMI
4339	Ittoqqortoormiit	70.48	-21.95	65/70	1961 ~ 2019	—	—	DMI
4250	Nuuk	64.17	-51.75	54/80	1961 ~ 2019	—	—	DMI
4270	Mitt.Narsarsuaq	61.17	-45.42	27	1961 ~ 2019	—	—	DMI
4272	Qaqortoq	60.72	-46.05	32	1961 ~ 2019	—	—	DMI
4360	Tasiilaq	65.6	-31.63	50	1961 ~ 2019	—	—	DMI
07	TUNU-N	78.02	-33.99	2113	1997 ~ 2017	—	—	GC-Net
12	NASA-E	75	-30	2631	1997 ~ 2017	—	—	GC-Net
01	Swiss Camp	69.57	-49.32	1149	1997 ~ 2017	—	—	GC-Net
06	Summit	72.58	-38.5	3254	1997 ~ 2017	—	—	GC-Net
08	DYE-2	66.48	-46.28	2165	1997 ~ 2017	—	—	GC-Net
—	Camp Century	77.17	-61.13	1885	9700B.C.E.~1960C.E.	1387	1966	Vinther,2009
—	NGRIP	75.1	-42.33	2917	9700B.C.E.~1960C.E.	3090	1996 ~ 2004	Vinther,2009
—	GRIP	72.58	-37.64	3230	9700B.C.E.~1960C.E.	3238	1993	Vinther,2009
—	GISP2	72.58	-38.48	3200	9700B.C.E.~1960C.E.	3208	1993	Stuiver,1995
—	Renland	71.3	-26.7	2350	9700B.C.E.~1960C.E.	325	1988	Vinther,2009
—	DYE-3	65.18	-43.83	2480	9700B.C.E.~1960C.E.	2037	1979 ~ 1981	Vinther,2009

159
160

3. Methods

161 In this study, the $\delta^{18}\text{O}$ value was converted into a specific temperature value by using the
162 conversion function method. A quantile mapping method was used to correct the bias between
163 monthly inland temperature observation data and ERA40 temperature data, and we employed
164 Pearson correlation analysis to measure the linear correlations between annual temperature and
165 monthly temperature at the same weather station, and the linear correlations of temperature between
166 adjacent meteorological stations. We also used linear regression equation to calculate the
167 relationship between annual temperature and monthly temperature, and residual correction method
168 was used to convert annual temperature data to monthly temperature data. Based on the spatial
169 distribution characteristics of ERA5 temperature data, the spatial distribution characteristics of
170 monthly temperature in the past ten thousand years were reconstructed.

3.1 Conversion function method

172 $\delta^{18}\text{O}$ record is a good proxy for environmental temperature, but the relationship between $\delta^{18}\text{O}$
173 and temperature is complicated, because many factors affect the isotopic composition, and these
174 factors are different in different climate (Cuffey and Clow, 1997). In this study, conversion functions
175 collected from many references were used to convert the $\delta^{18}\text{O}$ record into a specific temperature
176 value (cuffey et al., 1995; cuffey et al., 1997; Kapsner et al., 1995; Johnsen et al., 1995; Johnsen et
177 al., 1989), and we adjusted these functions to make the bias of temperature between this paper and
178 Buizert (2018) less than 3 °C.

3.2 Quantile-Mapping method

180 ERA40 is a global-scale raster dataset, and there exists bias between this dataset and true
181 temperature in local study area. In this study, we used Quantile-Mapping method to correct the bias.
182 It builds conversion function between meteorological observation data and reanalysis data according
183 to cumulative probability distribution function, and then we use the conversion function to correct
184 the reanalysis data in a different period. It has been used in temperature and precipitation data
185 correction, and the corrected results were better. And the commonly used quantile correction method
186 can be divided into two kinds of correction based on parameter method and non-parameter method.
187 If the meteorological observation data and reanalysis data satisfy hypothesis better, parameter

188 method can make a good result, or the results may be bad. And there is no hypothesis in non-
189 parameter method.

190 In this study, we used two parameter methods (namely, linear and scale method) and five non-
191 parameter methods (namely, QUANT-linear, QUANT-tricub, RQUANT-linear, RQUANT-tricub
192 and SSPLIN method) to build the conversion function between inland meteorological observation
193 data and ERA40 data during period 1995 ~ 1999, and the inland meteorological observation data
194 was used to verify the accuracy of the selected methods during period 2000 ~ 2001, but in 01 Swiss
195 Camp in year 2001. The methods with higher accuracy were selected to correct ERA40 temperature
196 data during the whole period 1958 ~ 2001 to acquire a high precision and long time series
197 temperature data in Greenland ice sheet. And the introduction of Quantile-Mapping method is in
198 this website: <http://127.0.0.1:14648/doc/html/Search?objects=1&port=14648>.

199 **3.3 Pearson correlation analysis**

200 The Pearson correlation analysis was used to measure the relationship between annual
201 temperature and monthly temperature, and the relationship of monthly temperature between coastal
202 weather stations and inland weather stations.

$$R = \frac{\sum_{i=1}^n (X_i - \bar{X})(Y_i - \bar{Y})}{\sqrt{\sum_{i=1}^n (X_i - \bar{X})^2} \sqrt{\sum_{i=1}^n (Y_i - \bar{Y})^2}} \quad (1)$$

203 where, R represents the Pearson correlation coefficient between X and Y, where 1, -1 and 0 reflect
204 a completely positive correlation, a completely negative correlation and no correlation, respectively,
205 between X and Y. The t-test method was used to determine the significance of the correlation
206 coefficient. X_i and Y_i reflect the variable values in year i, and \bar{X} and \bar{Y} are the corresponding mean
207 values.

208 **3.4 Linear Regression equation**

209 In this study, we used linear regression equation to build the relationship between annual
210 temperature and monthly temperature, and the equations were finally used to convert annual
211 temperature into monthly temperature.

$$Y = a + bx + \varepsilon \quad (2)$$

212 where, Y represents monthly temperature, x represents annual temperature, a is constant, b is

213 the slope of equation, ε is the random error.

214 **3.5 Model accuracy verification**

215 In this study, we used mean absolute error (MAE), root mean square error (RMSE) and
216 determination coefficient R^2 of validation dataset to evaluate the correction precision of quantile-
217 mapping method.

$$\text{MAE} = \left| \frac{\sum_{i=1}^n [\hat{Z}(x_i) - Z(x_i)]}{n} \right| \quad (3)$$

$$\text{RMSE} = \sqrt{\frac{\sum_{i=1}^n [\hat{Z}(x_i) - Z(x_i)]^2}{n}} \quad (4)$$

$$R^2 = 1 - \frac{\sum_{i=1}^n [\hat{Z}(x_i) - Z(x_i)]^2}{\sum_{i=1}^n [Z(x_i) - \bar{Z}(x_i)]^2} \quad (5)$$

218 where, n represents the numbers of samples in validation dataset, $\hat{Z}(x_i)$ represents the predicted
219 value, $Z(x_i)$ represents the observation value, $\bar{Z}(x_i)$ represent the mean of observation value.

220 The closer MAE is to 0, the method is unbiased. The smaller RMSE is, the higher prediction
221 accuracy is. The closer the R^2 is to 1, the better the model can explain the dependent variable.

222 **3.6 Time disaggregation method of temperature**

223 The temporal resolution of ice core data is year, we used linear regression equation to convert
224 the annual temperature into monthly temperature.

225 We firstly analyzed the correlation relationship between annual temperature and monthly
226 temperature, and the correlation relationship between coastal temperature and inland temperature.
227 If the correlation relationship between average annual temperature and monthly temperature is
228 significant, the linear regression equation between average annual temperature and monthly
229 temperature of coastal stations is established. If the correlation relationship between monthly mean
230 temperature of coastal stations and monthly mean temperature of inland stations is significant, the
231 above equation is applied to predict monthly mean temperature of inland stations. We calculated the
232 residuals between predicted temperature of inland stations and the corrected temperature of inland
233 ERA40 data, and we added the residuals when used the linear regression equation, and then we
234 verify the feasibility of the time disaggregation method. If the method is feasible, it is applied to

235 downscaling analysis of ice core temperature data.

236 **3.7 Construction of spatial distribution pattern of air temperature**

237 ERA5 is a global-scale raster dataset, it's not always accurate when used in a local study area.
238 In this study, we used the coastal temperature observation data and ERA5 temperature data to
239 construct the monthly temperature spatial distribution map. Firstly, we find the location of a coastal
240 weather station in the spatial distribution map of ERA5 data, and the adjacent eight raster point of
241 this location, we regard the mean temperature of ERA5 data of this nine raster points as the coastal
242 temperature, and then we calculated the coefficient between other raster temperature and the mean
243 temperature of this nine rasters, and thirdly, the temperature observation data of DMI coastal stations
244 were substituted and multiplied by the above coefficients to construct the spatial distribution map
245 of temperature.

246 **4. Results and discussion**

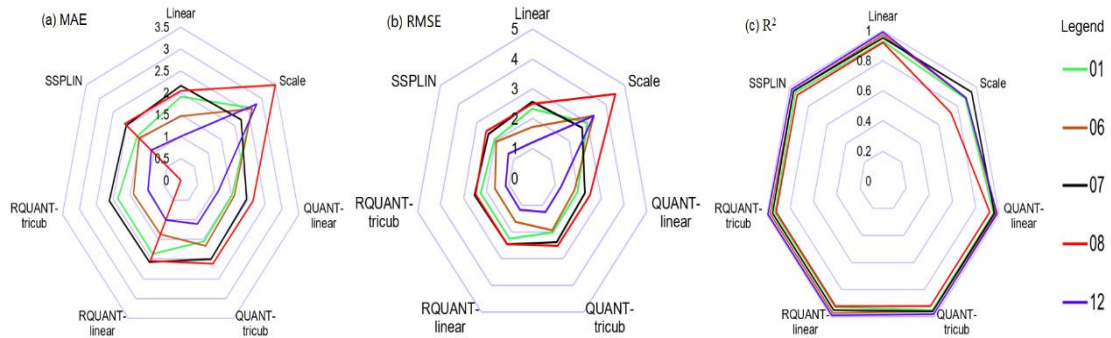
247 **4.1 Bias correction of ERA40 temperature data in Greenland ice sheet**

248 Fig. 2 shows the accuracy verification results of bias correction. From Fig. 2, we can see that
249 scale method has a bad accuracy in each weather station, it's not suitable for bias correction of
250 ERA40 temperature data, but linear, QUANT-linear, QUANT-tricub, RQUANT-linear, RQUANT-
251 tricub and SSPLIN method has the similar bias correction results, so we calculated the mean
252 temperature of these 6 methods as the final corrected temperature. As seen from Fig. 3, except for
253 12 NASA-E station, ERA40 temperature data corrected by quantile mapping method basically
254 coincided with the inland observation temperature data, while the performance of 12 NASA-E
255 station was poor, and the corrected ERA40 temperature data was higher than the observation
256 temperature.

257 Among the 6 methods selected, from the perspective of MAE, 01 Swiss Camp site is between
258 1.51 °C and 1.92°C, 06 Summit site is between 1.37 °C and 1.66°C, 07 Tunu-N site is between 1.94 °C
259 and 2.16°C, 08 Dye-2 station is between 0 and 2.14°C, and 12 NASA-E station is between 0.97 and
260 1.11°C. The ERA40 temperature after quantile mapping correction has a small bias from the inland
261 observation temperature, indicating that the corrected data has a certain reliability. From the
262 perspective of RMSE, 01 Swiss Camp site is between 1.99 °C and 2.34°C, 06 Summit site is between
263 1.63 °C and 1.96°C, 07 Tunu-N site is between 2.29 °C and 2.56°C, 08 Dye-2 station is between

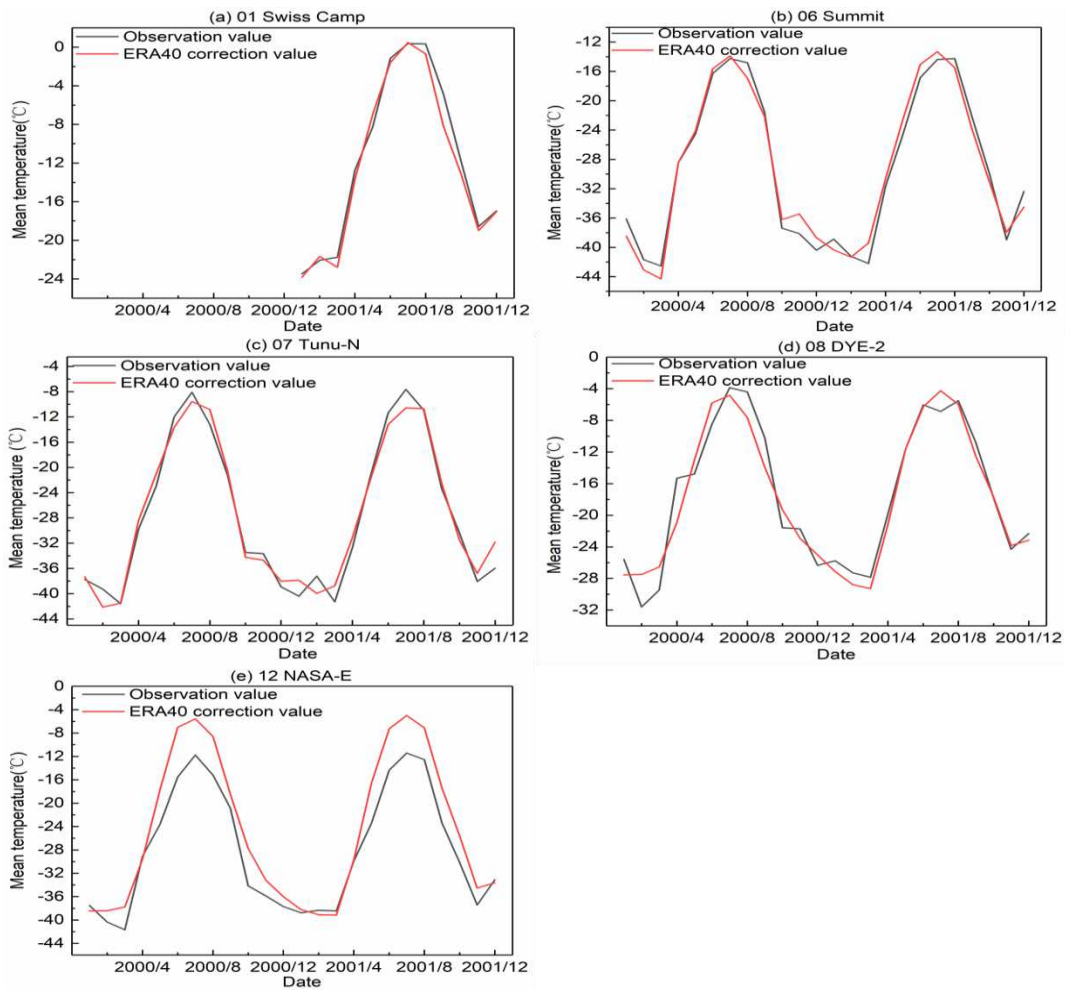
264 2.47 and 2.51°C, and 12 NASA-E station is between 1.16 and 1.31°C. The relatively small RMSE
 265 further illustrates the accuracy of the corrected results. From the perspective of R^2 , all 6 methods
 266 are above 0.91, indicates that the corrected results have a better accuracy.

267 From what has been discussed above, we selected 6 methods to correct ERA40 temperature,
 268 and the mean temperature of corrected ERA40 was used in this study.



269
 270

Fig. 2 Accuracy verification results of bias correction



271

272

Fig. 3 Comparison between observation temperature and ERA40 correction temperature

273 4.2 Correlation analysis of Greenland temperature

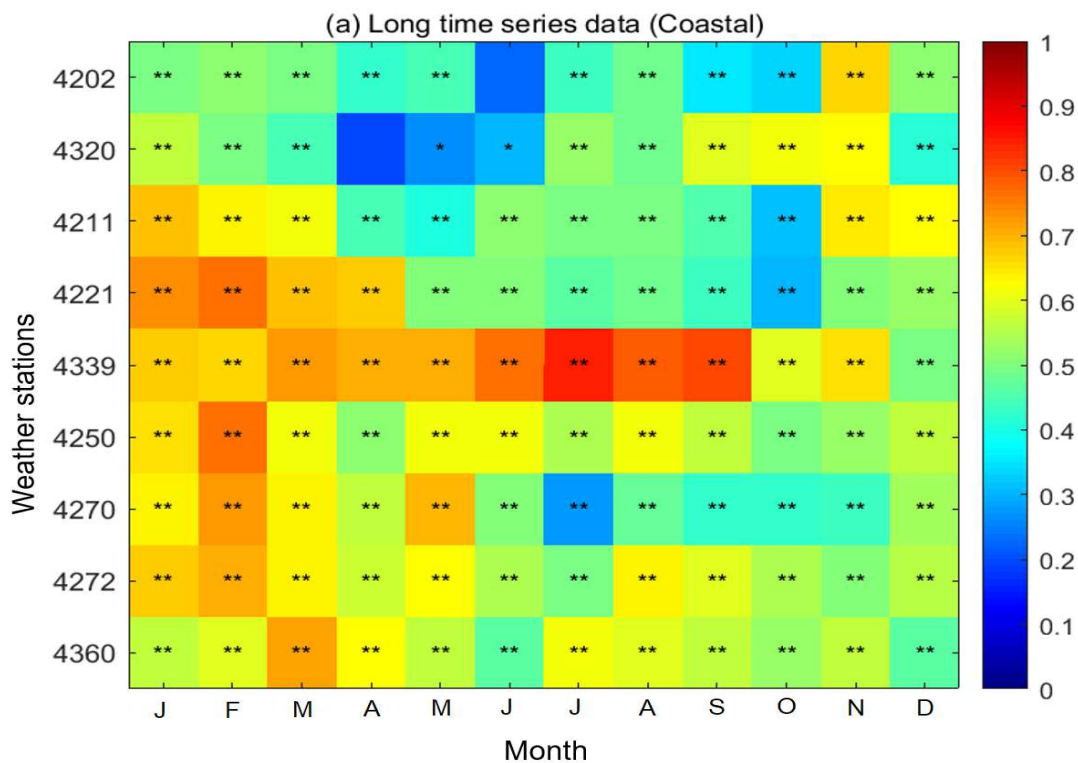
274 Fig. 4 shows the correlation relationship between annual average temperature and monthly
275 average temperature. As seen from Fig. 4a, annual average temperature and monthly average
276 temperature in coastal weather station are significantly correlated at the 0.01 level, and the
277 correlation coefficients ranged from 0.26 to 0.84. And the correlation coefficients from April to July
278 are lower than that from November to March in most weather stations, except 4339 weather station,
279 indicating that the average annual temperature is more affected by winter temperature fluctuation.
280 As seen from Fig. 4c, the correlation relationship between annual average temperature and summer
281 average temperature is not significant in 01 Swiss Camp, 06 Summit, 07 TUNU-N and 12 NASA-
282 E weather stations, and the annual average temperature are significantly correlated with other
283 months at the 0.01 level or 0.05 level, and the correlation coefficient is above 0.3. As for 08 DYE-
284 2 weather station, the correlation relationship between annual average temperature and April, May
285 and October temperature is not significant, and is significant with temperature of other months.

286 To discuss the effect of data length between annual average temperature and summer
287 temperature, we also analyzed the correlation relationship between annual average temperature and
288 monthly temperature in long time series data (time span: 1866 ~ 2019) and short time series data
289 (time span: 1958 ~ 2001) in coastal weather stations. As seen from Fig. 4a and Fig. 4b, the
290 correlation relationship may be insignificant from significant when the time span of data is
291 shortened from May to October, which means that the insignificant correlation relationship between
292 annual average temperature and summer temperature is caused by the data length, not data quality.

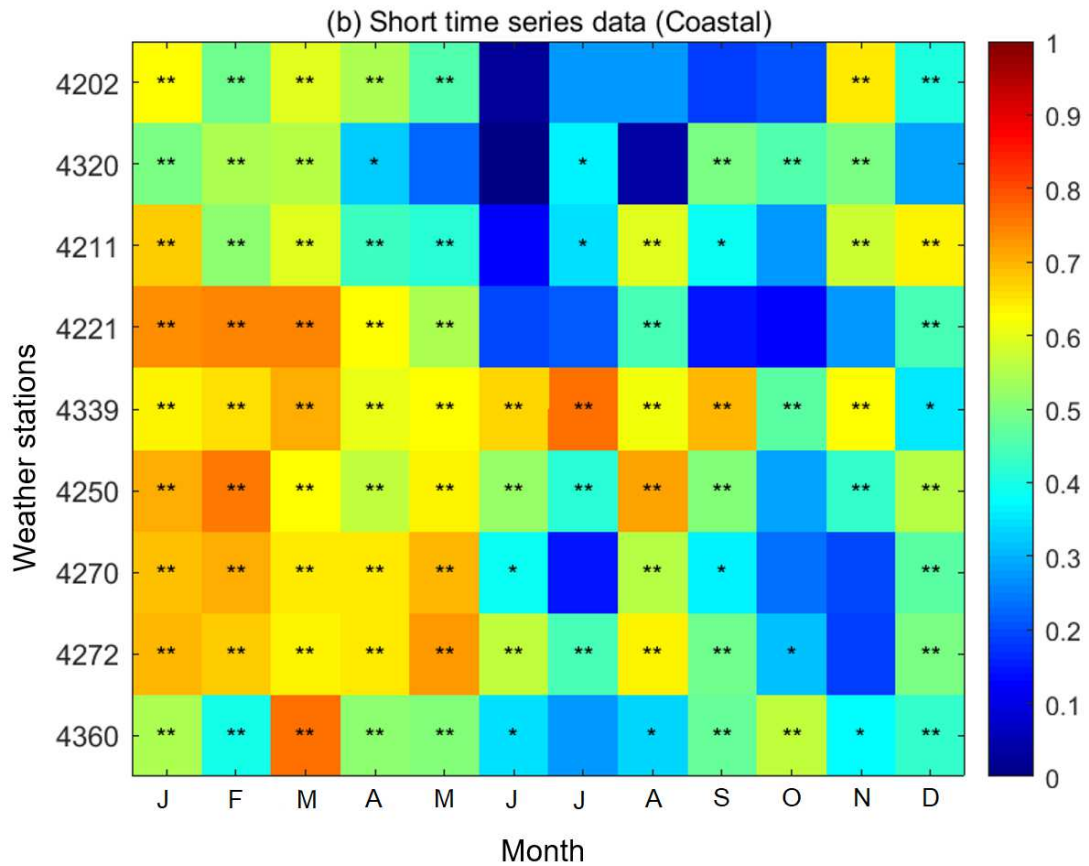
293 To reduce the impact of this phenomenon, the regression equation between annual average
294 temperature and monthly temperature of coastal stations was established in the disaggregation
295 analysis of air temperature, and the equation was applied to inland meteorological stations to be
296 adjusted according to residuals, and then the accuracy of disaggregation analysis was further
297 verified. Instead of establishing linear regression equation between average annual temperature and
298 monthly temperature of inland weather stations directly.

299 Fig. 5 shows the correlation relationship between coastal and inland temperature. In this study,
300 we selected the adjacent coastal weather station that the temperature of which has the highest
301 correlation coefficient with inland temperature, and the linear regression equation between annual

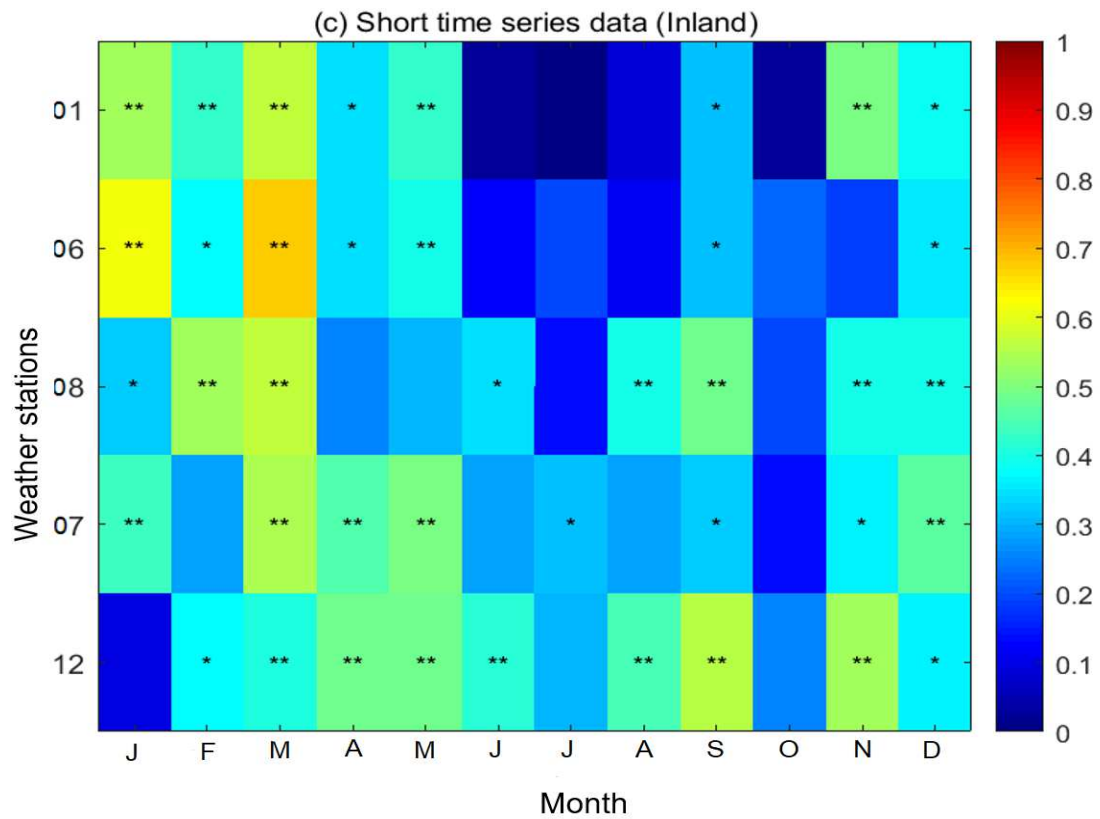
302 average temperature and monthly temperature of this selected station was used to predicted the
 303 monthly temperature of inland weather station, besides, we used residuals to adjust the predicted
 304 temperature. As seen from Fig. 5, weather station 4221 is close to weather station 01, and the
 305 monthly temperature of these two stations is significantly correlated at the level of 0.05, with the
 306 correlation coefficient ranging from 0.55 to 0.82. Therefore, the linear regression equation between
 307 annual average temperature and monthly temperature of weather station 4221 was used to predict
 308 the monthly temperature of weather station 01. In the same way, 4221, 4320,4360 and 4211 weather
 309 stations were selected, and the linear regression equation of them were used to predict the monthly
 310 temperature of 08, 12, 07 and 06 weather station, respectively. Besides, we also calculated the
 311 average temperature of all coastal weather stations, and the correlation relationship of temperature
 312 of inland weather station with it. As seen from Fig. 5, most monthly temperature of inland weather
 313 stations has a significantly correlation relationship with the average temperature of all coastal
 314 weather stations, and the correlation coefficient is above 0.3. Therefore, in this study, we used both
 315 linear regression equation of adjacent coastal weather station and the mean result of all coastal
 316 weather stations to predict inland temperature, and methods closer to inland temperature
 317 observations were selected for final disaggregation analysis.



318



319



320

321

Fig. 4 Correlation relationship between annual average temperature and monthly average

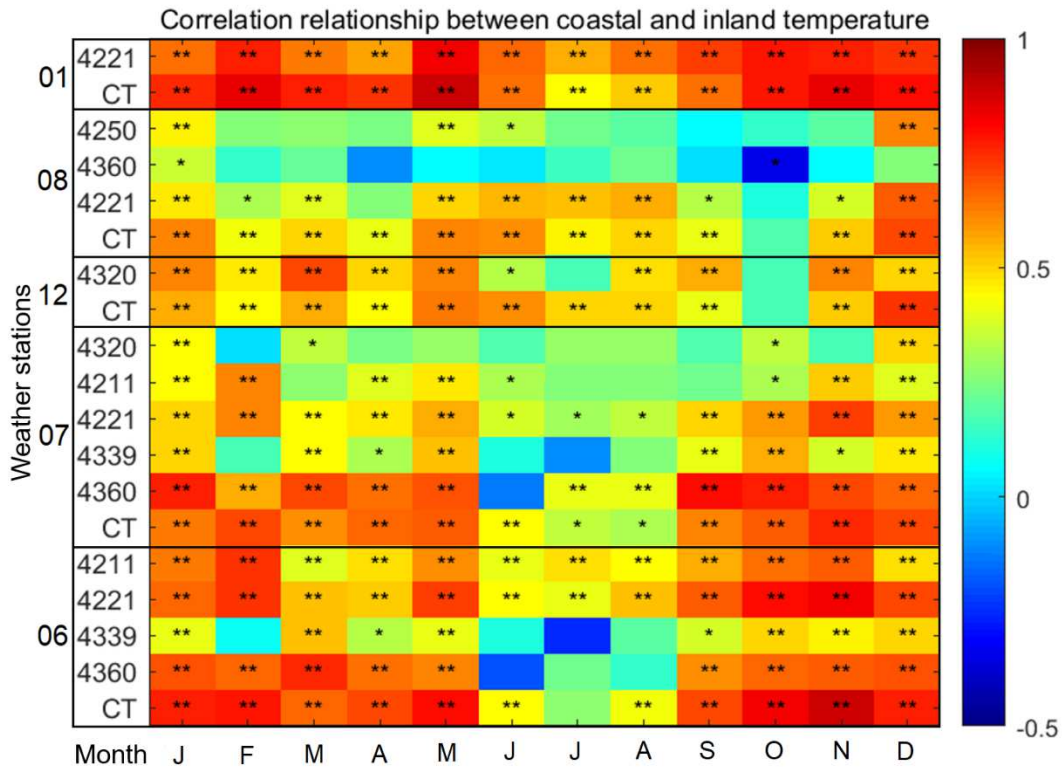
322

temperature. ** and * means that annual temperature and monthly temperature are significantly

323

correlated at 0.01 and 0.05 level, respectively. The longest time series data spans from 1866 to 2019,

324 and short time series data spans from 1958 to 2001. J, F, M, A, M, J, J, A, S, O, N, D represent the
 325 temperature of January to December.



326
 327 **Fig. 5** Correlation relationship between coastal and inland temperature. ** and * means that coastal
 328 temperature and inland temperature are significantly correlated at 0.01 and 0.05 level, respectively.
 329 CT is the average temperature of coastal weather stations. The column outside and inland of ordinate
 330 represents the temperature of inland and coastal stations, respectively.

331 **4.3 Time disaggregation equation of Greenland temperature**

332 Table 2 shows the regression equations between annual average temperature and monthly
 333 temperature of coastal weather stations. From Table 2, we can see that all equations were significant
 334 at $P < 0.001$, and the correlation coefficient R of equations range from 0.15 to 0.77, indicating that
 335 the equations can be well used to predict the monthly temperature of coastal weather stations.
 336 According to these equations, and the selected adjacent inland weather stations, the monthly
 337 temperature of inland weather stations can be predicted, but the predicted results needed to be
 338 adjusted by residuals, due to the differences of elevation between coastal and inland weather stations.
 339 In this study, we divided the corrected ERA40 temperature into two periods, period year 1971 ~
 340 2001 (namely, training set) and period year 1958 ~ 1970 (namely, validation set). And the training
 341 set was used to calculate the residuals between predicted inland monthly temperature by coastal

342 linear regression equation and corrected ERA40 monthly temperature data, the validation set was
343 used to verify the accuracy of linear regression equation-residual correction method. In this study,
344 we used the regional residuals not the station residuals. Stations 06, 12 and 07 are divided into a
345 group because they are close to each other, and the median of the residual errors of the three stations
346 was calculated as the residual correction of the monthly predicted temperature in central and
347 northern Greenland. And Station 06 is close to ice core station GISP2, GRIP and NGRIP, Therefore,
348 when downscaling the three ice core temperature data, the residual of 06 Summit site was selected
349 to correct the results of the regression equation. In the southern part of Greenland, 01 and 08 was
350 divided into a group, the median residual was calculated to correct the inland monthly mean
351 temperature predicted by the coastal regression equation.

352 Table 2 The regression equations between annual average temperature and monthly temperature of
353 coastal weather stations. J, F, M, A, M, J, J, A, S, O, N, D represent the temperature of January to
354 December, respectively, y represents annual average temperature. All equations are significant at P<
355 0.001.

Weather Station	Regression equation	R	Weather Station	Regression equation	R
4221	J=2.09×y-4.95	0.72	4320	J=1.90×y-0.15	0.55
	F=2.54×y-4.13	0.76		F=1.61×y-4.44	0.48
	M=1.82×y-6.22	0.68		M=1.15×y-9.29	0.42
	A=1.34×y-2.49	0.66		A=0.44×y-11.69	0.15
	M=0.57×y+2.83	0.50		M=0.44×y-1.36	0.23
	J=0.47×y+6.81	0.49		J=0.35×y+5.16	0.28
	J=0.33×y+9.00	0.45		J=0.51×y+9.88	0.51
	A=0.35×y+7.75	0.47		A=0.51×y+8.60	0.46
	S=0.36×y+3.91	0.42		S=0.86×y+6.34	0.58
	O=0.34×y-1.93	0.29		O=1.43×y+3.83	0.60
N=0.70×y-4.48	0.50	N=1.70×y+1.30	0.61		
D=1.09×y-6.07	0.51	D=1.14×y-7.99	0.40		
4360	J=1.57×y-5.51	0.57	4211	J=2.21×y-2.33	0.68
	F=1.71×y-5.97	0.58		F=1.97×y-6.18	0.63
	M=1.74×y-4.98	0.70		M=1.49×y-8.39	0.60
	A=1.21×y-2.08	0.61		A=0.81×y-6.80	0.43
	M=0.69×y+2.02	0.56		M=0.52×y+0.70	0.39
	J=0.42×y+5.31	0.45		J=0.51×y+5.52	0.51
	J=0.57×y+7.51	0.60		J=0.50×y+8.80	0.49
	A=0.52×y+6.91	0.58		A=0.48×y+8.42	0.49
	S=0.64×y+4.29	0.56		S=0.35×y+3.73	0.44
	O=0.81×y+0.32	0.51		O=0.32×y-1.57	0.30
N=1.07×y-2.87	0.56	N=1.08×y-0.78	0.63		
D=1.05×y-4.96	0.45	D=1.74×y-1.27	0.62		

	$J=1.86 \times y - 4.88$	0.69
	$F=1.95 \times y - 5.43$	0.69
	$M=1.61 \times y - 6.18$	0.70
	$A=0.88 \times y - 3.75$	0.58
	$M=0.71 \times y + 2.34$	0.63
CT	$J=0.53 \times y + 6.16$	0.59
	$J=0.48 \times y + 8.44$	0.52
	$A=0.67 \times y + 8.63$	0.77
	$S=0.48 \times y + 4.15$	0.56
	$O=0.63 \times y - 0.53$	0.50
	$N=0.87 \times y - 3.87$	0.56
	$D=1.34 \times y - 5.09$	0.58

356

357

4.4 Accuracy verification of Greenland monthly temperature disaggregation result

358

Fig. 6 shows the accuracy of time disaggregation result in inland weather stations. From the perspective of MAE during period from 1971 to 2001 (Fig. 6a), the MAE of 01 Swiss Camp, 08 Dye-2 and 06 Summit sites was the smallest in July, which gradually decreased from January to July and increased from July to December. However, MAE at 12 NASA-E and 07 TUNU-N sites did not show an obvious change pattern, and the MAE of these 5 sites ranges from 0.58 to 4.66°C.

359

360

361

362

363

364

365

366

367

368

369

370

371

372

373

374

375

376

377

The MAE in 12 NASA-E is larger, it may be related to the poor bias correction results of 12 NASA-E sites (Fig. 3), with MAE around 3°C at other sites. From the perspective of RMSE (Fig. 6c), which has a similar change pattern with MAE, the RMSE of 01 Swiss Camp, 08 Dye-2 and 06 Summit weather stations was the smallest in July, which gradually decreased from January to July and increased from July to December. However, RMSE at 12 NASA-E and 07 TUNU-N sites did not show an obvious change pattern, and RMSE in these 5 weather stations ranges from 0.76 ~ 5.04 °C. Because the poor bias correction of 12 NASA-E, the RMSE in 12 NASA-E station is the largest. From the perspective of R (Fig. 6e), the prediction of temperature in Winter is better than that in Summer, and R in these 5 weather stations range from 0.01 to 0.64, R in some months is very smaller, this is in normal. Because we used the regional residuals to adjust the inland prediction of monthly temperature not the residuals of one weather station when we used the coastal linear regression equation between annual average temperature and monthly temperature, leading to a lower R.

We selected the data set during period 1958 ~ 1970 to validate the accuracy of linear regression equation-residual correction method. From Fig. 6b, Fig. 6d, Fig. 6f, we can see that the accuracy is lower than period 1971 ~ 2001. As shown from Fig. 6b, MAE in 5 weather stations ranges from

378 0.57 to 4.86 °C, and MAE in 12 NASA-E is poor, too. MAE is larger from October to March than
 379 that from April to September, indicating that the accuracy of linear regression equation-residual
 380 correction method is better in Summer than Winter. As shown from Fig. 6d, RMSE in 5 weather
 381 stations range from 0.71 to 5.28 °C. And RMSE has a similar change pattern with MAE, which is
 382 larger from October to March than that from April to September. As shown from Fig. 6f, R in 5
 383 weather stations ranges from -0.23 to 0.84, which is similar with R during period 1971 ~ 2001. But
 384 there are some negative values of R, this may be affected by regional residuals, which needed to be
 385 improved in future work. From the accuracy of validation set, linear regression equation-residual
 386 correction method can be well used in Greenland to predict monthly temperature of inland weather
 387 stations. In the next analysis, we used the linear regression between annual average temperature and
 388 monthly temperature of coastal weather stations to predict monthly temperature of ice cores in
 389 Greenland ice sheet, and residuals correction method was used to acquire accurate results.

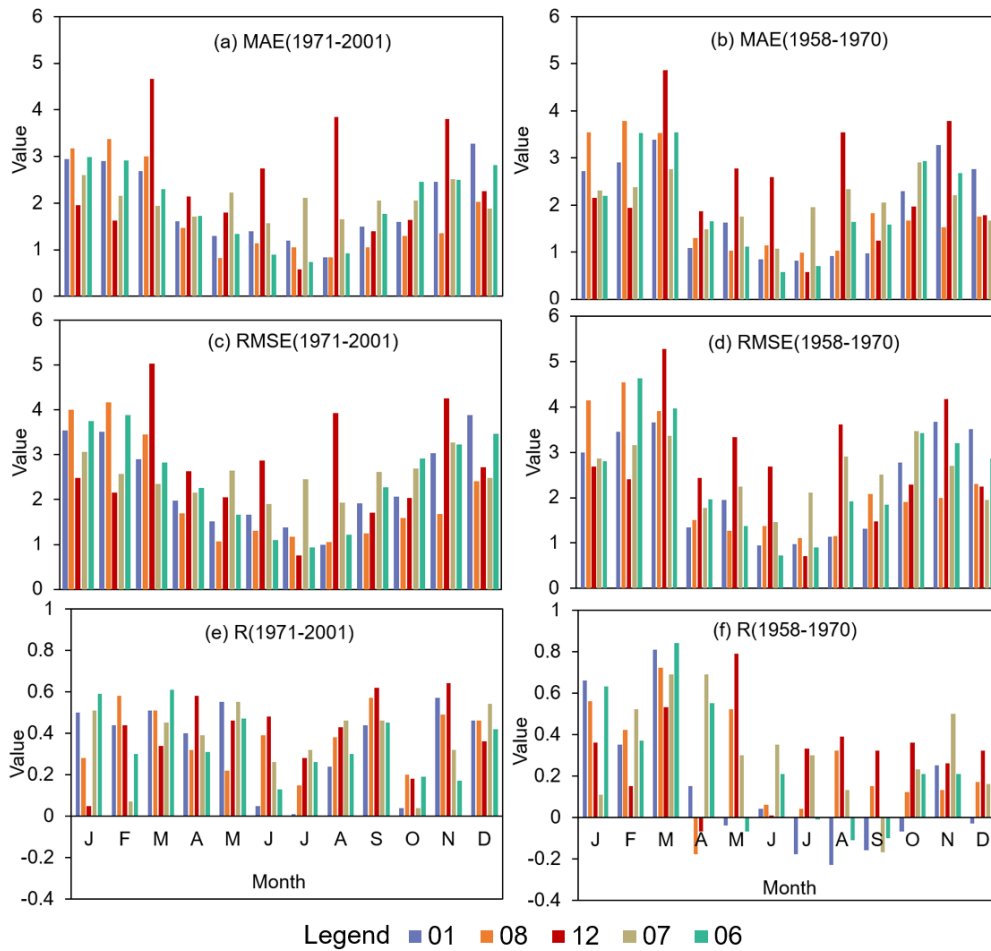


Fig. 6 Accuracy verification of disaggregation result in inland weather stations

392 **4.5 Comparison with other temperature reconstruction results**

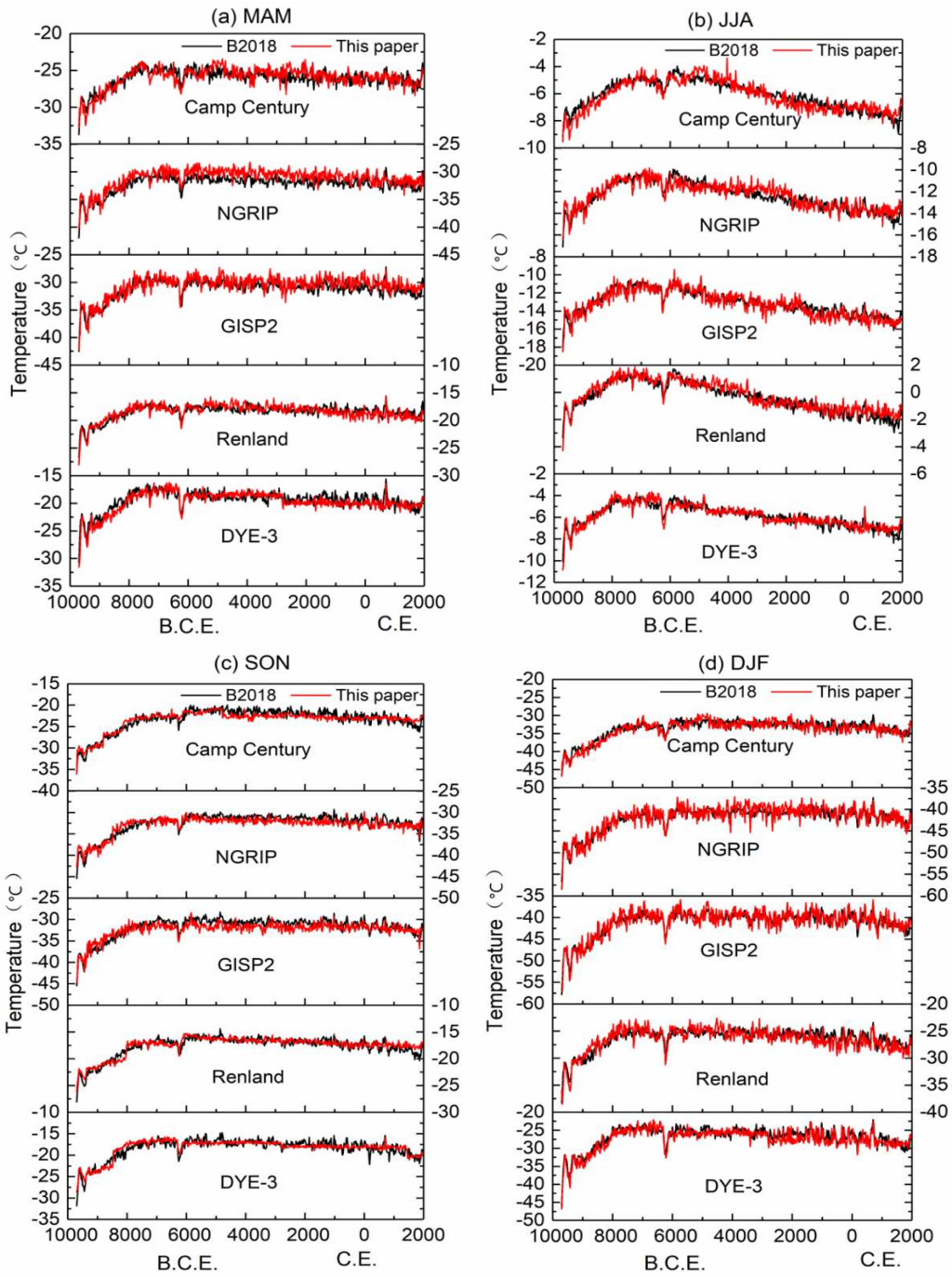
393 In this study, we used linear regression equation- residuals correction method to reconstruct
394 the monthly temperature of Greenland ice core data. The bias of reconstructed monthly temperature
395 between our results and Buizert's results (2018) is less than 3 °C.

396 Buizert (2018) used temperature proxy index N^{15} to reconstruct average annual temperature of
397 ice core data, and the reconstructed error of average annual temperature of NGRIP, GISP2 and
398 NEEM ice core is about 3 °C, and the error in Holocene is 1.5°C. And they used meteorological
399 observation data combining with regional climate modeling method to reconstruct seasonal
400 temperature, and the error of reconstructed seasonal temperature ranges from 1.4 to 2 °C.

401 As seen from Fig. 7, there exists about 3 °C bias between our results and Buizert's result due
402 to the use of different temperature proxy index and different temperature reconstructing method.
403 But both results can describe temperature change characteristic over past 10 000 years, such as the
404 temperature change characteristic in Little Ice Age, Holocene Thermal Maximum, 8.2 ka event and
405 11.3 ka event.

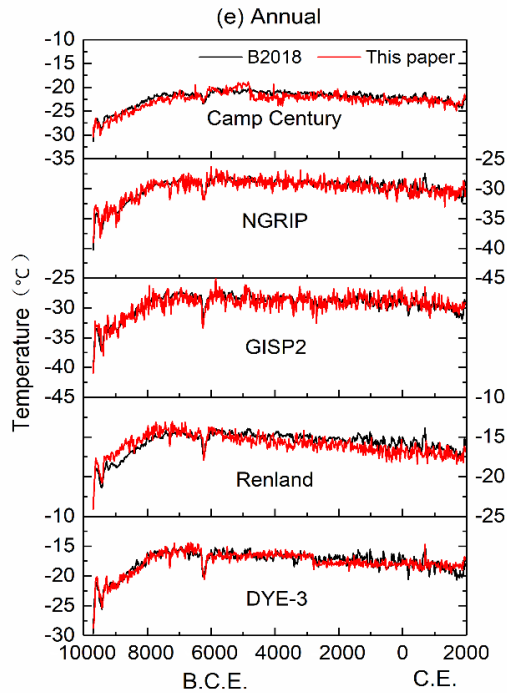
406 As seen from Fig. 7, the Little Ice Age, 8.2 ka and 11.3 ka events were three Holocene cooling
407 events. The Little Ice Age event occurred during period 1820 C.E. ~ 860 C.E., and the minimum
408 average annual temperature of Camp Century, NGRIP, GRIP, GISP2, Renland and DYE-3 is -
409 24.94 °C, -33.08 °C, -31.24 °C, -31.69 °C, -18.43 °C and -19.55 °C, respectively. And the minimum
410 monthly temperature of these 6 ice cores is -38.49 °C, -47.22 °C, -47.23 °C, -46.64 °C, -32.29 °C, and
411 -33.28 °C, respectively. 8.2 ka event occurred during period 6220 B.C.E. ~ 6260 B.C.E., and the
412 minimum average annual temperature of Camp Century, NGRIP, GRIP, GISP2, Renland and DYE-
413 3 is -23.36 °C, -31.90 °C, -32.52 °C, -33.42 °C, -17.94 °C and -20.58 °C, respectively, and the
414 minimum monthly temperature of these 6 ice cores is -38.66 °C, -47.94 °C, -48.26 °C, -48.01 °C, -
415 33.34 °C and -35.47 °C, respectively. 11.3 ka event occurred during period 9400 B.C.E. ~ 9480
416 B.C.E., and the minimum average annual temperature of Camp Century, NGRIP, GRIP, GISP2,
417 Renland and DYE-3 is -30.15 °C, -38.24 °C, -33.93 °C, -38.02 °C, -20.81 °C, and -25.39 °C,
418 respectively. And the minimum monthly temperature of these 6 ice cores is -44.79 °C, -55.12 °C, -
419 55.84 °C, -57.70 °C, -38.93 °C and -44.87 °C, respectively. Holocene Thermal Maximum was a
420 period of high temperature, and the average annual temperature of Camp Century, NGRIP, GRIP,

421 GISP2, Renland and DYE-3 is $-21.62\text{ }^{\circ}\text{C}$, $-28.97\text{ }^{\circ}\text{C}$, $-29.10\text{ }^{\circ}\text{C}$, $-28.69\text{ }^{\circ}\text{C}$, $-14.80\text{ }^{\circ}\text{C}$ and $-16.43\text{ }^{\circ}\text{C}$,
422 respectively.



423

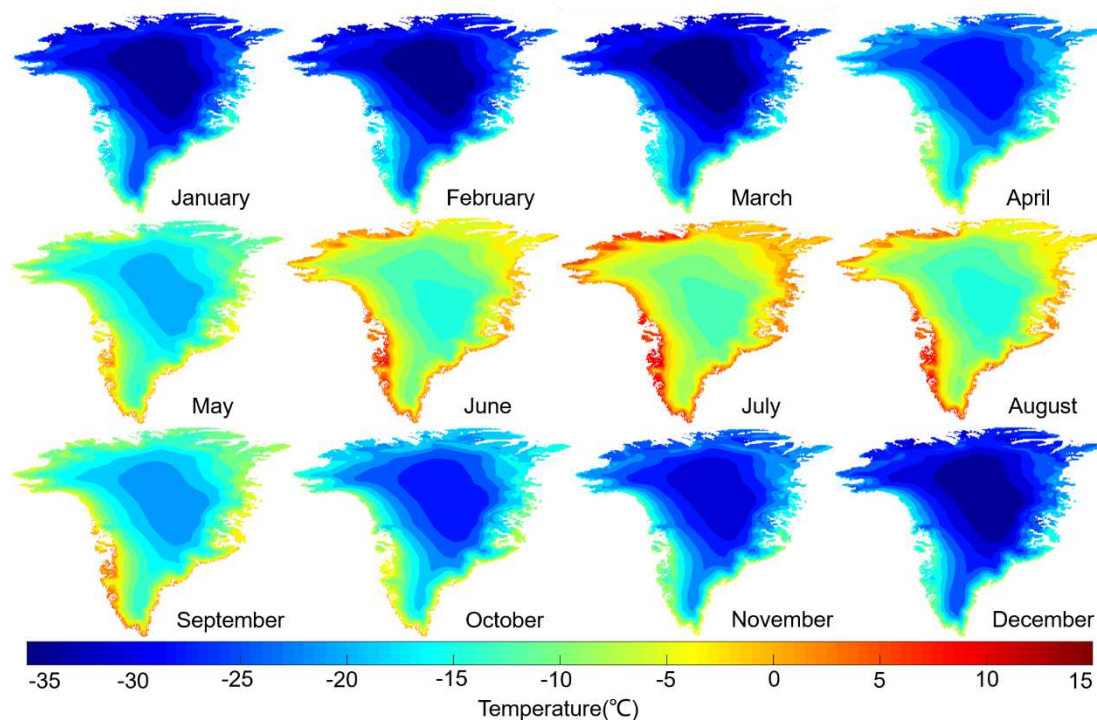
424



425
 426 **Fig. 7** Comparison between reconstructed temperature in this study and Buizert (2018). B2018
 427 represents the reconstructed temperature of Buizert, 2108.

428 **4.6 The spatial distribution pattern of Greenland monthly temperature**

429 In this study, we used coastal meteorological observation data and ice core data combing with
 430 ERA5 data to construct the temperature spatial distribution map of Greenland. As seen from Fig. 8,
 431 the spatial distribution characteristic of temperature in Greenland has obvious elevation effect,that
 432 is, the temperature decreases gradually with the increase of elevation.The temperature increases
 433 gradually from the north to the southregion.And temperature decreases gradually from the east to
 434 the west region from November to April, while the temperature change from May to October is
 435 opposite to that from November to April. The monthly average temperature of the whole island is -
 436 22.63°C (January), -23.22°C (February), -23.45°C (March), -18.04°C (April), -10.79°C (May), -
 437 5.24°C (June), -2.87°C (July), -4.68°C (August), -10.38°C (September), and -15.82°C (October), -
 438 19.20°C (November) and -21.76°C (December), respectively. The results of temperature
 439 construction in this study are in good agreement with the spatial distribution of temperature
 440 constructed by Fausto et al. (2009).



441 **Fig. 8** Spatial distribution map of average Greenland monthly temperature during period 1961-2019

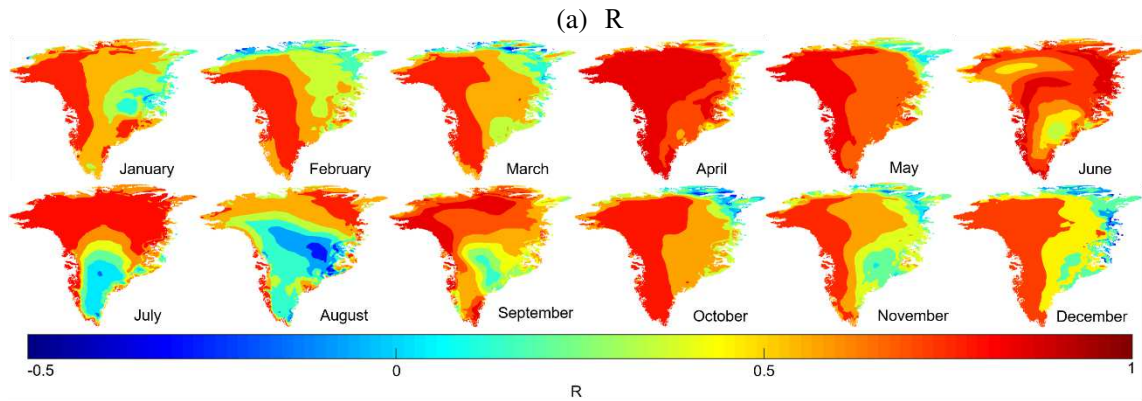
442 **4.7 Verify the accuracy of monthly temperature spatial distribution map**

443 In order to verify the accuracy of monthly temperature spatial distribution map of Greenland,
 444 ERA5 temperature data from 1981 to 2010 were selected for modeling, and data from 2011 to 2020
 445 were used for verification, and evaluation methods of R, MAE and RMSE were selected to verify
 446 the feasibility.

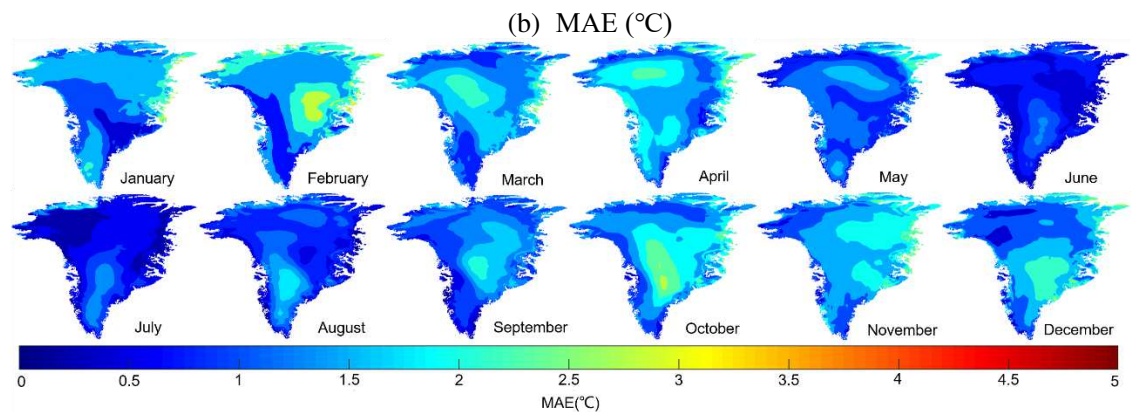
447 As seen from Fig. 9, monthly correlation coefficient R of the island is between 0.54 ~ 0.77,
 448 among them, some regions of R is negative, these value are in the northern, northeastern and east-
 449 central region of the island, because there are little weather stations in these regions. From the
 450 respective of MAE, the average MAE of the island is between 0.76 ~ 2.07°C, it means that the bias
 451 between predicted temperature and observation temperature is lower, the predicted temperature map
 452 has higher accuracy. From the spatial distribution map of MAE, the higher bias is in the regions of
 453 higher altitudes, because of sparse weather stations. From the respective of RMSE, the average
 454 RMSE of the between 0.92 ~ 2.64°C, it means that the predicted temperature map has higher
 455 accuracy.

456
 457
 458
 459

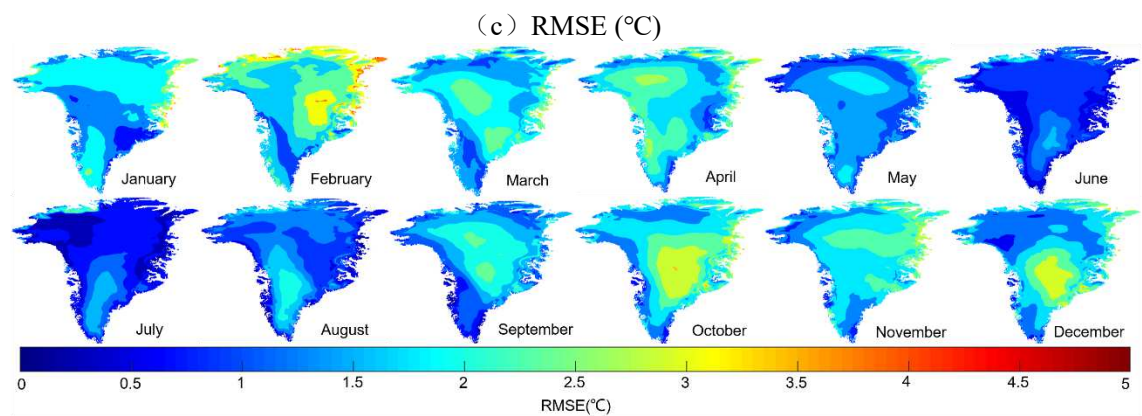
460



461
462



463
464



465
466

Fig. 9 Verify the accuracy of spatial distribution map of monthly temperature

467

From what has been discussed above, the average bias of predicted temperature spatial distribution map of the island is about 2 °C, which has higher predicted accuracy. And the predicted accuracy in the higher altitudes is lower because of sparse weather stations.

470

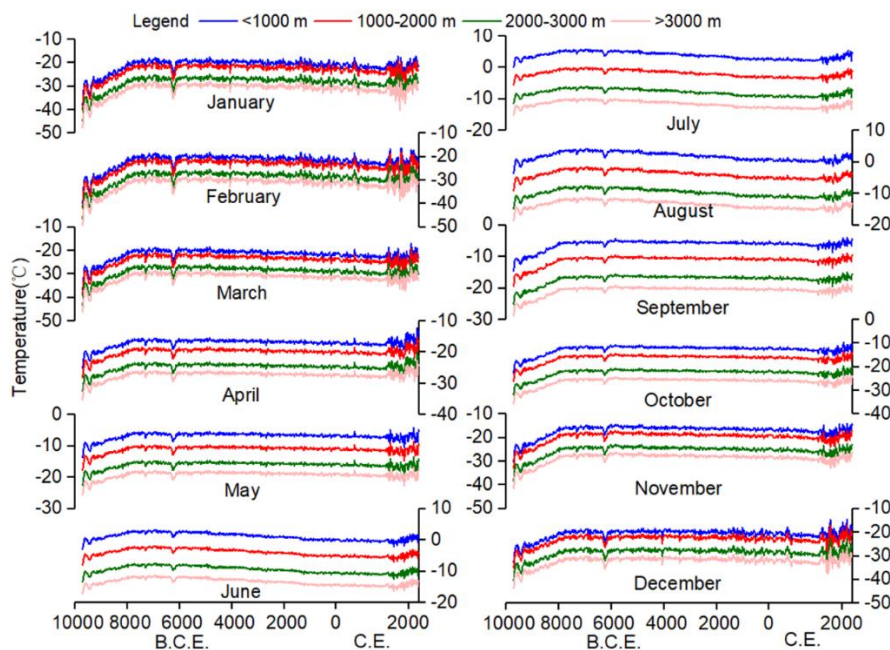
4.8 The temporal variation characteristic of reconstructed monthly temperature

471

In order to analyze the variation characteristics of air temperature from 9700 B.C.E. to 2019 C.E., according to the spatial distribution map of air temperature constructed above, air temperature is greatly affected by elevation. This paper divides the study area into four sub-regions according to elevation. That is, the elevation of 9 ~ 1 000, 1 000 ~ 2 000, 2 000 ~ 3 000 and 3 000 ~ 3 673 m, respectively, and the temporal variation characteristics of monthly temperature were analysed.

475

476 As seen from Fig. 10, from 9700 B.C.E. to 2019 C.E., the air temperature from September to
 477 May of the next year showed a significant increasing trend at the 0.05 level, while the air
 478 temperature from June to August showed a significant decreasing trend at the 0.05 level. During the
 479 whole period, the temperature change can be divided into 9 periods. Table 3 lists the slope of
 480 temperature change for each period. As seen from Fig. 10 and Table 3, from 9700 B.C.E. to 9600
 481 B.C.E., the temperature in each elevation region showed an obvious upward trend, and the
 482 temperature rising rate in this period was the most obvious among all periods. From 9600 B.C.E. to
 483 9400 B.C.E., the temperature at all elevation regions showed a decreasing trend, which was
 484 consistent with the cooling event time of 11.3 ka. Then, from 9400 B.C.E. to 7720 B.C.E., the
 485 temperature gradually increased until 7720 B.C.E. to 6340 B.C.E., the temperature remained almost
 486 constant or showed a slight decreasing trend. 8.2 ka event (6340 B.C.E. ~ 6240 B.C.E.) was the most
 487 severe cooling event in the last 10 000 years. Then, from 6240 B.C.E. TO 6000 B.C.E., the
 488 temperature began to rise gradually. From 6000 B.C.E. to 1800 C.E., the temperature showed a
 489 decreasing trend. From 1800 C.E. to 2019 C.E., the temperature showed an upward trend. And the
 490 slope difference of temperature change in the same period and month in different elevation areas is
 491 not obvious. The reconstructed in our study is consist with previous work (Badgeley et al., 2020;
 492 Polyakov et al., 2002; McKay et al., 2014; Buizert et al., 2018; Kobashi et al., 2017), indicating that
 493 the reconstructed temperature of our study has high reliability.



494
 495

Fig. 10 Temporal variation characteristic of monthly temperature over past 10,000 years.

Table 3 The slope of temperature change during different periods (°C per two decades). Region 1 ~ 4 represent elevation region 9 ~ 1000 m, 1000 ~ 2000 m,

2000 ~ 3000 m and 3000 ~ 3673 m, respectively. The minus sign represents B.C.E., and the unmarked sign represents C.E.

Reg.	Period	Jan	Feb	Mar	Apr	May	Jun	Jul	Aug	Sep	Oct	Nov	Dec
1	-9700~2019	0.0056	0.0058	0.0034	0.0021	0.0018	-0.0040	-0.0040	-0.0037	0.0039	0.0043	0.0051	0.0040
	1800~ 2019	0.1622	0.1725	0.0503	0.1344	0.0120	0.0541	0.0997	0.0804	0.0785	0.0618	0.0751	0.2198
	-6000~1800	-0.0072	-0.0077	-0.0075	-0.0036	-0.0028	-0.0086	-0.0084	-0.0094	-0.0028	-0.0036	-0.0053	-0.0044
	-6240~-6000	0.5421	0.5748	0.4972	0.2591	0.2154	0.1630	0.1481	0.2078	0.1665	0.2172	0.3334	0.3704
	-6340~-6240	-1.2985	-1.3715	-1.1384	-0.6098	-0.5156	-0.3861	-0.3540	-0.4860	-0.3513	-0.4642	-0.7317	-0.9162
	-7720~-6340	0.0000	0.0000	0.0000	-0.0032	-0.0038	0.0000	0.0000	0.0000	0.0019	0.0025	0.0036	-0.0029
	-9400~-7720	0.1184	0.1252	0.1051	0.0561	0.0473	0.0357	0.0327	0.0450	0.0702	0.0809	0.1053	0.0830
	-9600~-9400	-0.6502	-0.6876	-0.6158	-0.3446	-0.2962	-0.1977	-0.1813	-0.2489	-0.1544	-0.2121	-0.3487	-0.4545
-9700~-9600	2.2247	2.3614	2.1466	1.1504	0.9693	0.7258	0.6644	0.9137	0.7558	0.9684	1.4598	1.5063	
2	-9700~2019	0.0056	0.0058	0.0034	0.0020	0.0017	-0.0039	-0.0039	-0.0036	0.0039	0.0042	0.0050	0.0046
	1800~ 2019	0.1602	0.1708	0.0494	0.1332	0.0119	0.0531	0.0976	0.0788	0.0770	0.0609	0.0743	0.2178
	-6000~1800	-0.0072	-0.0077	-0.0074	-0.0036	-0.0028	-0.0085	-0.0082	-0.0092	-0.0027	-0.0036	-0.0053	-0.0044
	-6240~-6000	0.5378	0.5704	0.4929	0.2562	0.2120	0.1599	0.1451	0.2035	0.1634	0.2141	0.3298	0.3670
	-6340~-6240	-1.2883	-1.3610	-1.1286	-0.6029	-0.5074	-0.3789	-0.3467	-0.4759	-0.3447	-0.4576	-0.7239	-0.9078
	-7720~-6340	0.0000	0.0000	0.0000	-0.0032	-0.0038	0.0000	0.0000	0.0000	0.0018	0.0025	0.0035	-0.0028
	-9400~-7720	0.1175	0.1242	0.1042	0.0555	0.0465	0.0351	0.0320	0.0440	0.0689	0.0797	0.1042	0.0823
	-9600~-9400	-0.6452	-0.6824	-0.6105	-0.3406	-0.2915	-0.1941	-0.1775	-0.2438	-0.1515	-0.2090	-0.3450	-0.4503
-9700~-9600	2.2073	2.3435	2.1281	1.1374	0.9540	0.7123	0.6507	0.8947	0.7416	0.9547	1.4443	1.4925	
3	-9700~2019	0.0055	0.0057	0.0033	0.0020	0.0017	-0.0038	-0.0038	-0.0035	0.0038	0.0041	0.0049	0.0045
	1800~ 2019	0.1549	0.1664	0.0475	0.1313	0.0116	0.0520	0.0954	0.0770	0.0753	0.0595	0.0726	0.2129
	-6000~1800	-0.0070	-0.0075	-0.0073	-0.0035	-0.0027	-0.0083	-0.0080	-0.0090	-0.0027	-0.0035	-0.0052	-0.0043
	-6240~-6000	0.5267	0.5588	0.4831	0.2514	0.2080	0.1567	0.1419	0.1990	0.1596	0.2090	0.3224	0.3588
	-6340~-6240	-1.2617	-1.3333	-1.1062	-0.5917	-0.4978	-0.3711	-0.3390	-0.4655	-0.3368	-0.4466	-0.7076	-0.8876
	-7720~-6340	0.0000	0.0000	0.0000	-0.0031	-0.0037	0.0000	0.0000	0.0000	0.0018	0.0024	0.0034	-0.0028
	-9400~-7720	0.1151	0.1217	0.1022	0.0545	0.0456	0.0343	0.0313	0.0431	0.0674	0.0778	0.1018	0.0804

	-9600~-9400	-0.6318	-0.6685	-0.5984	-0.3343	-0.2860	-0.1901	-0.1736	-0.2384	-0.1480	-0.2041	-0.3372	-0.4403
	-9700~-9600	2.1616	2.2957	2.0860	1.1162	0.9359	0.6978	0.6362	0.8751	0.7247	0.9319	1.4117	1.4592
	-9700~2019	0.0054	0.0056	0.0033	0.0020	0.0017	-0.0037	-0.0038	-0.0035	0.0037	0.0040	0.0049	0.0044
	1800~ 2019	0.1520	0.1640	0.0465	0.1302	0.0115	0.0512	0.0941	0.0760	0.0742	0.0586	0.0716	0.2098
	-6000~1800	-0.0069	-0.0074	-0.0072	-0.0035	-0.0027	-0.0082	-0.0079	-0.0089	-0.0026	-0.0034	-0.0051	-0.0042
4	-6240~-6000	0.5205	0.5525	0.4779	0.2487	0.2054	0.1544	0.1399	0.1962	0.1574	0.2059	0.3182	0.3536
	-6340~-6240	-1.2469	-1.3184	-1.0943	-0.5853	-0.4917	-0.3657	-0.3343	-0.4590	-0.3321	-0.4400	-0.6983	-0.8746
	-7720~-6340	0.0000	0.0000	0.0000	-0.0031	-0.0037	0.0000	0.0000	0.0000	0.0018	0.0024	0.0034	-0.0027
	-9400~-7720	0.1137	0.1203	0.1011	0.0539	0.0451	0.0338	0.0309	0.0425	0.0664	0.0767	0.1005	0.0793
	-9600~-9400	-0.6244	-0.6610	-0.5920	-0.3307	-0.2825	-0.1873	-0.1712	-0.2351	-0.1460	-0.2010	-0.3328	-0.4338
	-9700~-9600	2.1363	2.2700	2.0635	1.1042	0.9244	0.6876	0.6273	0.8628	0.7145	0.9181	1.3932	1.4379

499 **4.9 Discussion**

500 Due to the limitations of data and methods, there are some errors in the reconstruction of
501 monthly temperature in Greenland. The possible error sources mainly include the following three
502 aspects: the error of converting ice core proxy indicator into actual temperature, the error of
503 constructing spatial distribution map of temperature, and the downscaling error of temperature.

504 $\delta^{18}\text{O}$ is usually used as a temperature proxy to analyze the characteristics of temperature
505 changes in Greenland during the past ten thousand years. The $\delta^{18}\text{O}$ is converted into the actual
506 temperature by using the conversion function method. There exists deviation between the converted
507 temperature value and the real temperature value, which cannot be measured at present. The
508 temperature deviation between the converted temperature and Buizert temperature in this study is
509 within 3°C. In addition, $\delta^{18}\text{O}$ can produce some errors during laboratory measurements (Vinther et
510 al., 2006; Stuiver and Grootes, 2000), this paper ignores this error.

511 In order to analyze the spatial variation characteristics of air temperature in Greenland, we
512 constructed a spatial distribution map based on the spatial distribution characteristics of ERA5 air
513 temperature in Greenland, and substituted the data of coastal meteorological stations and ice cores.
514 According to the accuracy verification results, the average monthly MAE of the temperature spatial
515 distribution map of the whole island is between 0.76 °C and 2.07°C.

516 The downscaling method of temperature was adopted by linear regression equation - residual
517 correction method. Among this, the deviation between the temperature reconstructed by this method
518 and the reconstructed temperature by Buizert is within 3°C.

519 Due to the lack of real temperature data, quantitative analysis of reconstruction errors of
520 temperature and precipitation in Greenland is a difficult problem. This paper makes a simple
521 comparison based on existing literature, which can be strengthened in future studies.

522 **5. Conclusions**

523 Polar climate change and its influence on sea level and sea ice has been a hot topic in recent
524 years. We took Greenland as a study area in this study, reconstructed the monthly temperature
525 dataset over past 10,000 years, and analyzed the monthly temperature change characteristic of
526 Greenland. And from the reconstructed results, we can make the following conclusions:

527 The temperature of September to May showed a significant increasing trend at the 0.05 level

528 during period 9700 B. C. E. ~ 2019 C.E., and the increasing rate is 0.0017 ~ 0.0058 °C every two
529 decades. However, the temperature of June to August showed a significant decreasing trend, and the
530 decreasing rate is -0.0035 ~ -0.0040 °C every two decades. But the reconstructed results exist 3 °C
531 bias compared with Buizert's reconstructed results. In the future, data assimilation method can be
532 used to reduce the uncertainty of the reconstruction results in combination with the climate model
533 simulation data.

534 **Acknowledgments**

535 This study was supported by the Natural Science Foundation of China (No. 51879009,
536 41875131, 42171022), the Second Tibetan Plateau Scientific Expedition and Research Program
537 (No.2019QZKK0405), the National Key Research and Development Program of China (No.
538 2018YFE0196000).

539 **Data Availability Statement**

540 The monthly coastal meteorological observation data in Greenland was downloaded from
541 Danish Meteorological Institute (DMI), and the website is: <https://www.dmi.dk/publikationer/>. The
542 ice cores data were downloaded from NOAA paleoclimatology data website, and the website is:
543 <https://www.ncdc.noaa.gov/data-access/paleoclimatology-data/datasets>. And the ERA40 and ERA5
544 data were downloaded from the following website: [https://apps.ecmwf.int/datasets/data/era40-](https://apps.ecmwf.int/datasets/data/era40-mnth/levtype=sfc/)
545 [mnth/levtype=sfc/](https://apps.ecmwf.int/datasets/data/era40-mnth/levtype=sfc/) and [https://cds.climate.copernicus.eu/cdsapp#!/dataset/reanalysis-era5-land-](https://cds.climate.copernicus.eu/cdsapp#!/dataset/reanalysis-era5-land-monthly-means?tab=overview)
546 [monthly-means?tab=overview](https://cds.climate.copernicus.eu/cdsapp#!/dataset/reanalysis-era5-land-monthly-means?tab=overview).

547

548 **References**

Badgeley J A, Steig E J, Hakim G J, Fudge T J (2020) Greenland temperature and precipitation over
the last 20 000 years using data assimilation. *Clim Past* 16(4): 1325-1346. doi: 10.5194/cp-16-
1325-2020

Buizert C, Keisling B A, Box J E, He F, Carlson A E, Sinclair G, DeConto R M (2018) Greenland-
wide seasonal temperatures during the last deglaciation. *Geophys Res Lett* 45: 1905-1914. doi:
10.1002/2017GL075601

Cohen J, Screen J A, Furtado J C, Barlow M, Whittleston D, Coumou D, Francis J, Dethloff K,

- Entekhabi D, Overland J, Jones J (2014) Recent Arctic amplification and extreme mid-latitude weather. *Nature Geosci* 7(9): 627-637. doi: 10.1038/ngeo2234
- Cuffey K M, Clow G D (1997) Temperature, accumulation, and ice sheet elevation in central Greenland through the last deglacial transition. *J Geophys Res Atmos* 102(C12): 26383-26396. doi: 10.1029/96JC03981
- Cuffey K M, Clow G D, Alley R B, Stuiver M, Waddington E D, Saltus R W (1995) Large arctic temperature change at the Wisconsin-Holocene glacial transition. *Science* 270(5235): 455-458. doi: 10.1126/science.270.5235.455
- Johnsen S J, Dahl-Jensen D, Gundestrup N, Steffensen J P, Clausen H B, Miller H, Masson-Delmotte V, Sveinbjornsdottir A E, White J (2001) Oxygen isotope and palaeotemperature records from six Greenland ice-core stations: Camp Century, Dye-3, GRIP, GISP2, Renland and NorthGRIP. *J Quaternary Sci* 16(4): 299-307. doi: 10.1002/jqs.622
- Johnsen S J, Dahl-Jensen D, Dansgaard W, Gundestrup N (1995) Greenland palaeotemperatures derived from GRIP bore hole temperature and ice core isotope profiles. *Tellus B: Chem and Phys Meteo* 47(5): 624-629. doi: 10.1034/j.1600-0889.47.issue5.9.x
- Johnsen S J, Dansgaard W, White, J, W C (1989) The origin of Arctic precipitation under present and glacial conditions. *Tellus* 41(4): 452-468. doi: 10.3402/tellusb.v41i4.15100
- Kapsner W R, Alley R B, Shuman C A, Anandakrishnan S, Grootes P M (1995) Dominant influence of atmospheric circulation on snow accumulation in Greenland over the past 18,000 years. *Nature* 373: 52-54. doi: 10.1038/373052a0
- Kobashi T, Menviel L, Jeltsch-Thömmes A, Vinther B M, Box J. E, Muscheler R, Nakaegawa T, Pfister P L, Döring M, Leuenberger M, Wanner H, Ohmura A (2017) Volcanic influence on centennial to millennial Holocene Greenland temperature change. *Sci Rep-UK* 7(1): 1-10. doi: 10.1038/s41598-017-01451-7
- Kobashi T, Severinghaus J P, Barnola J M, Kawamura K, Carter T, Nakaegawa T (2010) Persistent multi-decadal Greenland temperature fluctuation through the last millennium. *Clim Change* 100(3-4): 733-756. doi: 10.1007/s10584-009-9689-9
- McKay N P, Kaufman D S (2014) An extended Arctic proxy temperature database for the past 2,000

- years. *Sci Data* 1: 140026. doi: 10.1038/sdata.2014.26
- Polyakov I V, Alekseev G V, Bekryaev R V, Bhatt U, Colony R. L, Johnson M A, Karklin V P, Makshtas A P, Walsh D, and Yulin A V (2002) Observationally based assessment of polar amplification of global warming. *Geophys Res Lett* 29 (18): 1878. doi:10.1029/2001GL011111
- Saiping J, Aizhong Y, Cunde Xiao (2020) The temperature increase in Greenland has accelerated in the past five years. *Global Planet Change* 194, 103297. doi: 10.1016/j.gloplacha.2020.103297
- Steffen K, Box J E (2001) Surface climatology of the Greenland Ice Sheet: Greenland Climate Network 1995-1999. *J Geophys Res Atmos* 106(D24): 33951-33964. doi: 10.1029/2001JD900161
- Steffensen J P, Andersen K K, Bigler M, Clausen H B, Dahl-Jensen D, Fischer H, Goto-Azuma K, Hansson M, Johnsen S J, Jouzel J, Masson-Delmotte V, Popp T, Rasmussen SO, Röthlisberger R, Ruth U, Stauffer B, Siggaard-Andersen M-L, Sveinbjörnsdóttir AE, Svensson A, White JW.C (2008) High-resolution Greenland ice core data show abrupt climate change happens in few years. *Science* 321(5889): 680-684. doi: 10.1126/science.1157707
- Stuiver M, Grootes P M (2000) GISP2 oxygen isotope ratios. *Quaternary Res* 53(3), 277-284. doi: 10.1006/qres.2000.2127
- Vinther B M, Clausen H B, Johnsen S J, Rasmussen S O, Andersen K K, Buchardt S L, Dahl-Jensen D, Seierstad I K, Siggaard-Andersen M - L, Steffensen J P, Svensson A, Olsen J, Heinemeier J (2006) A synchronized dating of three Greenland ice cores throughout the Holocene. *J Geophys Res* 111(D13102). doi: 10.1029/2005JD006921